Figure S1

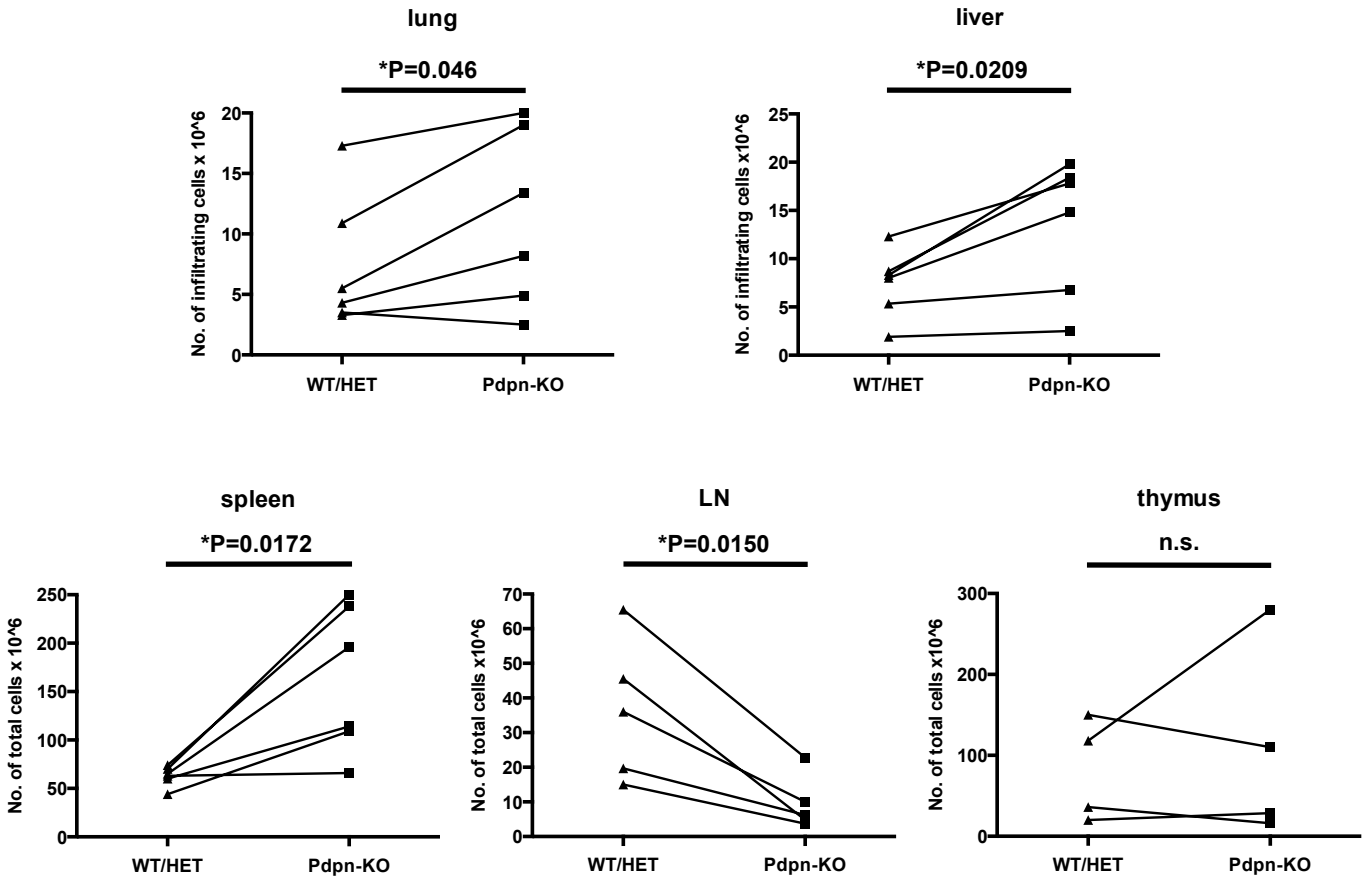

Figure S1. Pdpn-deficient mice develop inflammatory infiltrates in multiple organs
Lung, liver, spleen, lymph nodes / lymph node remnants, and thymus were harvested from Pdpn-deficient mice and their wild type or heterozygous littermates. Mononuclear cells were isolated from lung and liver and single cell suspensions were made from spleen, lymph nodes / lymph node remnants, and thymus. Live cells were counted via Trypan Blue exclusion. Data points connected with lines represent littermates. Differences between groups were tested for significance using a paired Student's *t*-test.

Figure S2

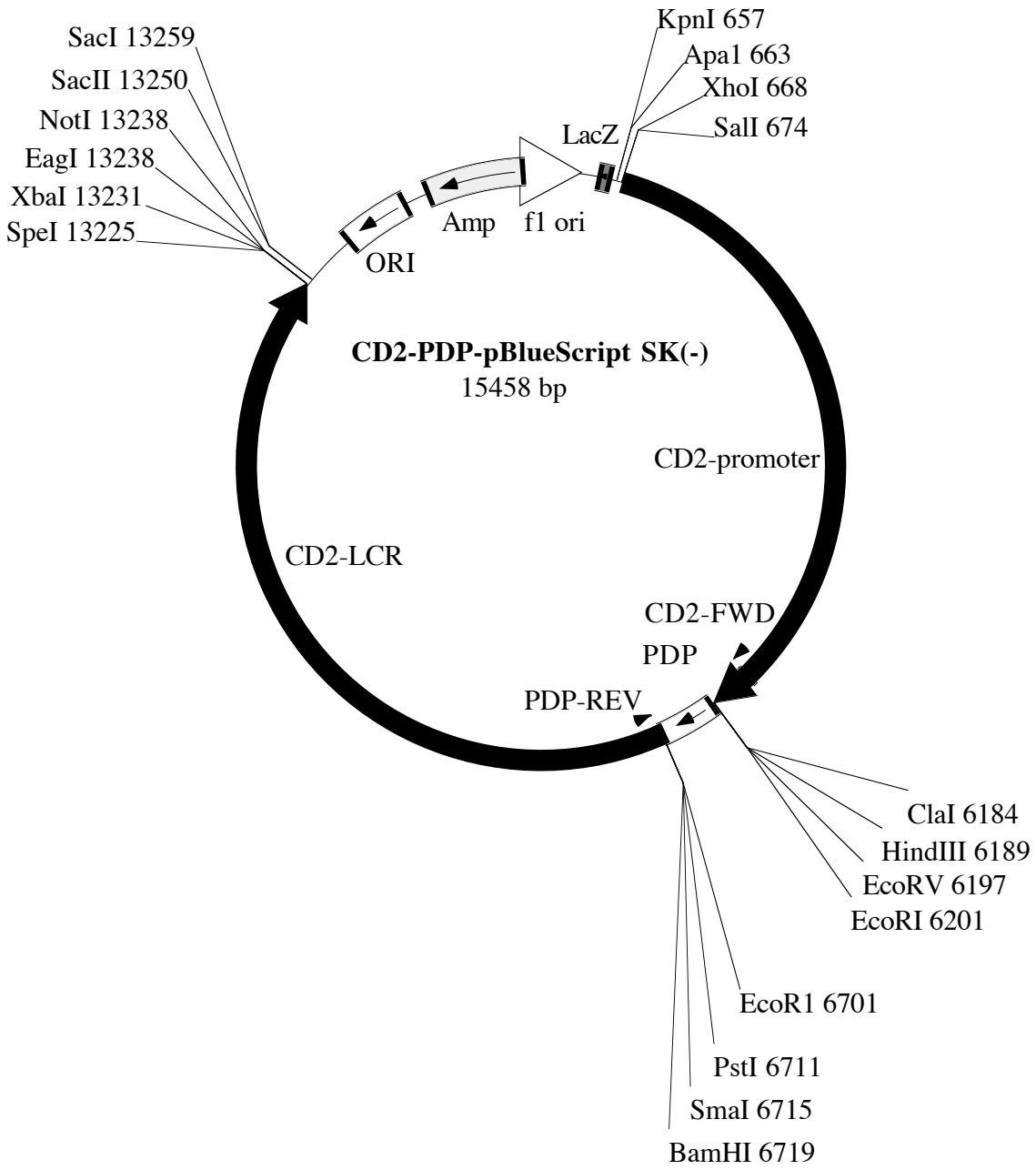

Figure S2. Generation of PdpnTG mice
Pdpn cDNA was cloned into a human CD2 expression cassette using the EcoRI site. After sequencing and digestion with NotI and SalI the construct was purified and microinjected directly into C57BL/6 oocytes.

Figure S3

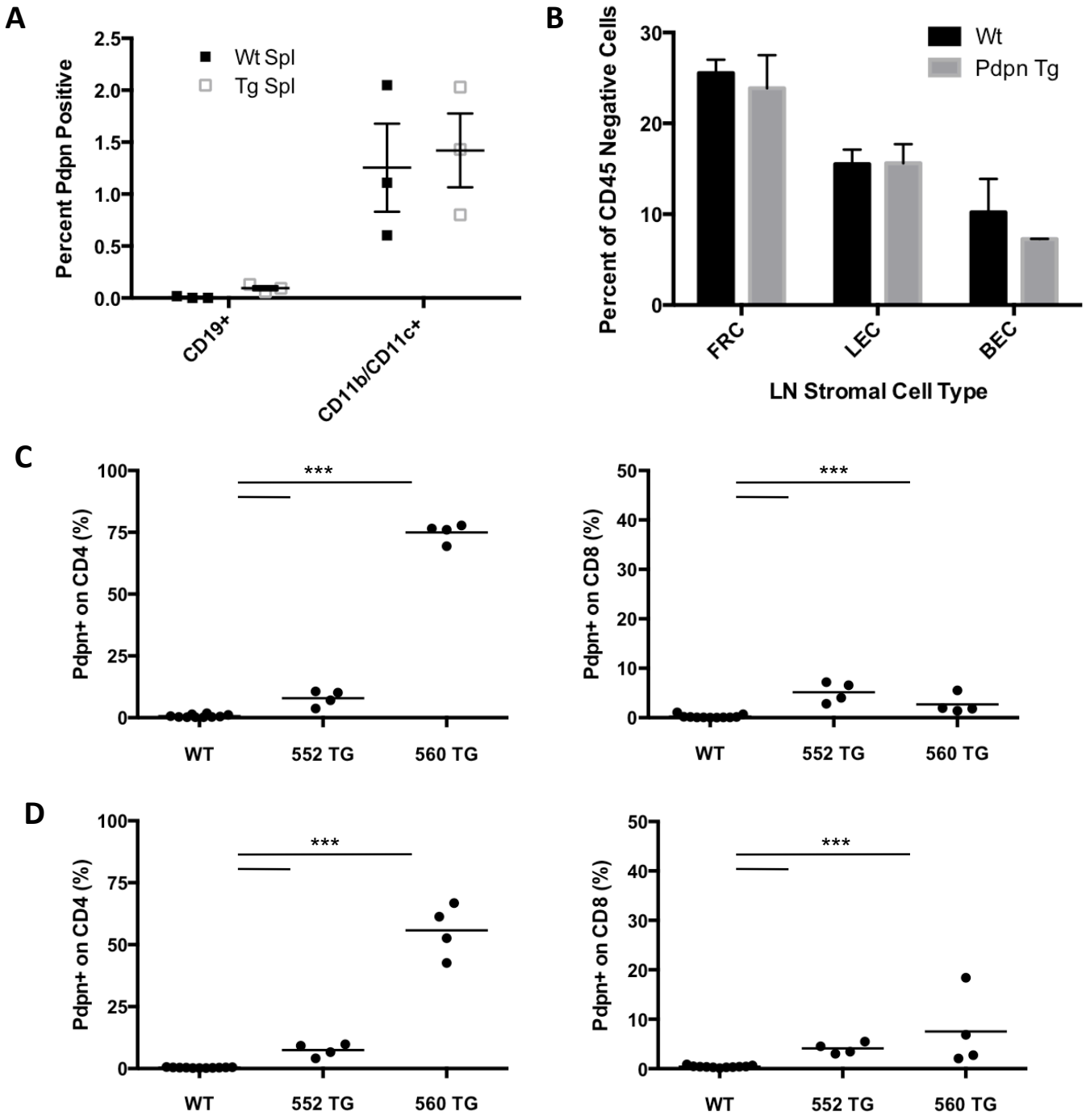

Figure S3. Pdpn expression levels on different cell types from PdpnTG mice
(A) Splenic CD19+ B cells and CD11b/CD11c+ myeloid cells from WT and PdpnTG mice (line 560) were analyzed for Pdpn expression by flow cytometry. **(B)** The frequencies of lymph node stromal cell populations including fibroblastic reticular cells (FRC), lymphatic endothelial cells (LEC) and blood endothelial cells (BEC) in WT and PdpnTG (line 560) mice were analyzed by flow cytometry. **(C-D)** Lymph nodes and spleen were harvested from two independent lines of 6-12 week old PdpnTG mice and their WT littermates. **(C)** CD4 (left panel) and CD8 T cells (right panel) from lymph nodes were analyzed for expression of Pdpn by flow cytometry. **(D)** CD4 (left panel) and CD8 T cells (right panel) from spleen were analyzed for expression of Pdpn by flow cytometry. Data points represent individual mice. Differences between groups were tested for significance using an unpaired Student's *t*-test (***P<0.001).

Figure S4

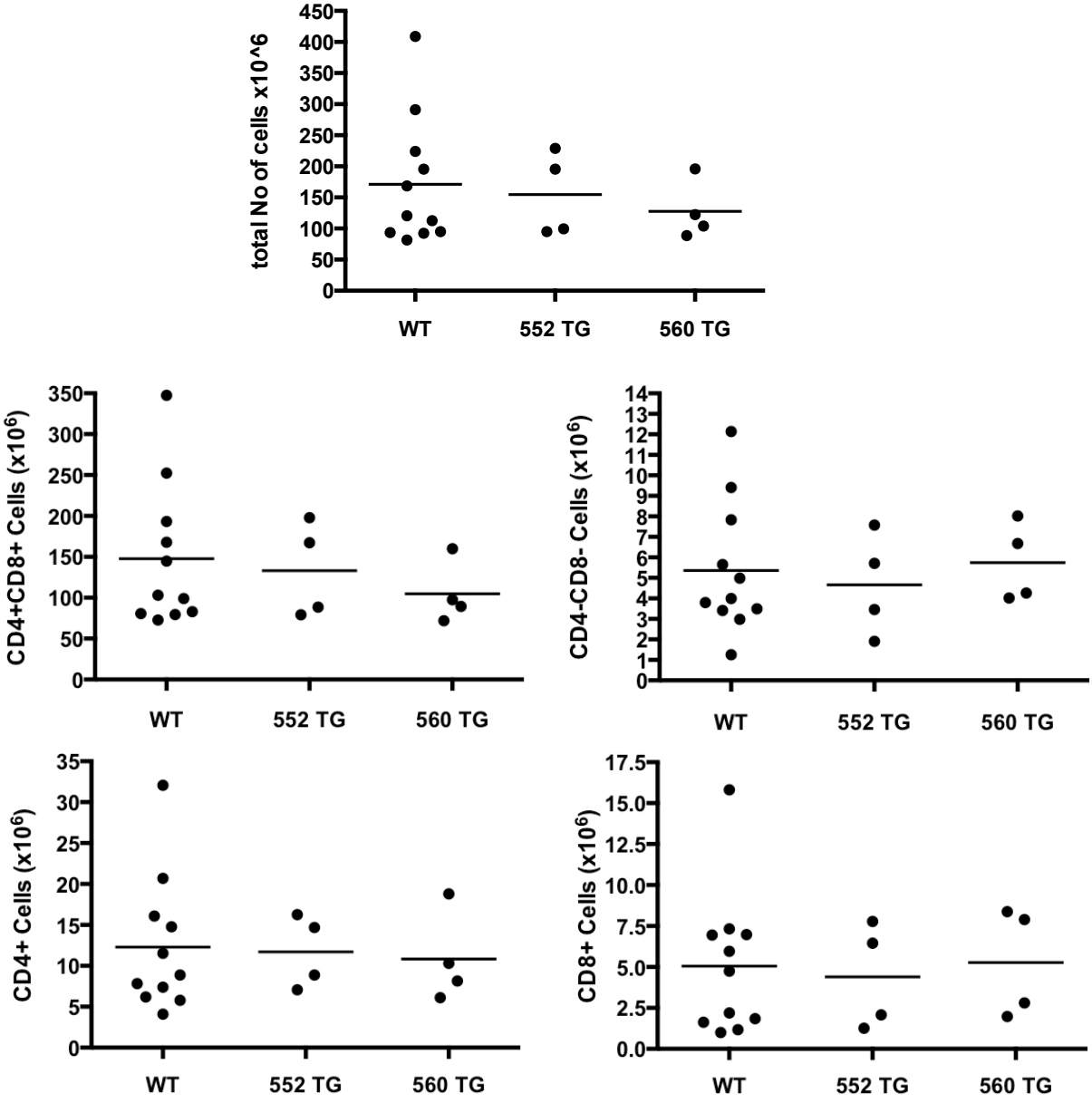

Figure S4. Characterization of thymic T cell populations in PdpnTG mice
Thymuses were harvested from two independent lines of 6-12 week old PdpnTG mice and their WT littermates and live cells in single cell suspension were counted via Trypan Blue exclusion (upper plot). Cells were the analyzed for presence and total number of CD4+CD8+ (middle left), CD4-CD8- (middle right), CD4+CD8- (lower left) and CD4-CD8+ T cell populations (lower right) by flow cytometry. Data points represent individual mice.

Figure S5

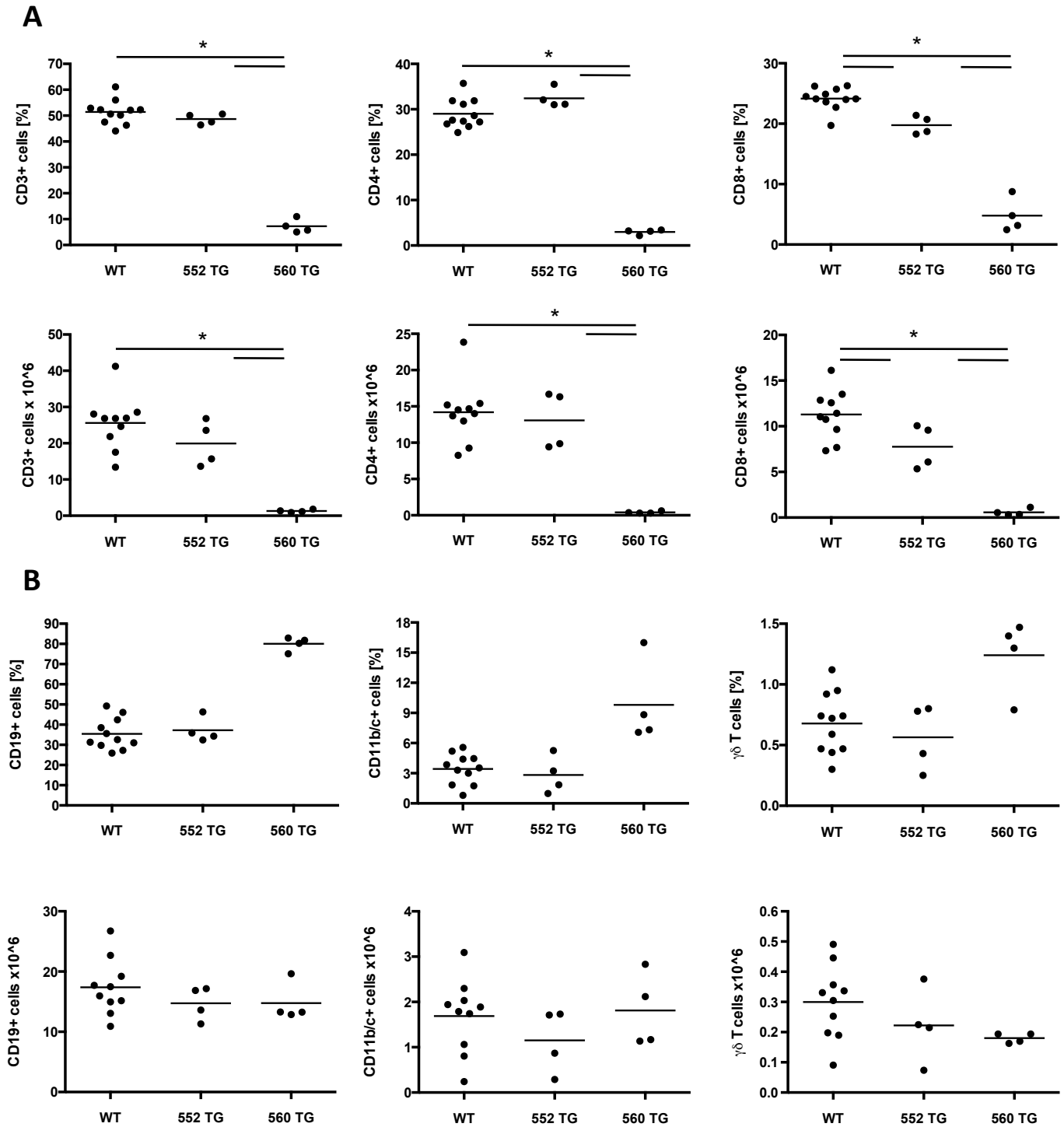

Figure S5. Characterization of different cell types in PdpnTG mice

(A-B) Lymph nodes were harvested from two independent lines of 6-12 week old PdpnTG mice and their WT littermates. Single cell suspensions were made and live cells were counted by Trypan Blue exclusion. (A) Single cell suspensions were analyzed for frequency (upper panels) and total number (lower panels) of CD3 (left), CD4 (middle), and CD8 (right) T cells by flow cytometry. Differences between groups were tested for significance using an unpaired Student's *t*-test (*P<0.01). **(B)** Single cell suspensions were analyzed for frequency (upper panel) and total number (lower panel) of CD19+ (left), CD11b/c+ (middle), and TCR$\gamma\delta$+ (right) cells by flow cytometry.

Figure S6

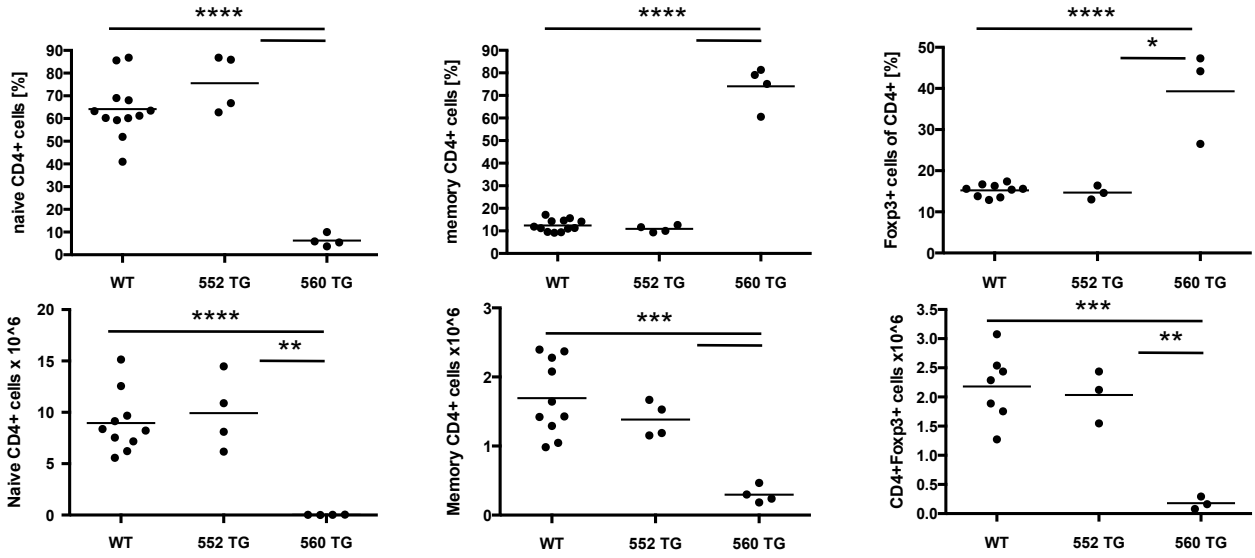

Figure S6. Altered composition of the peripheral T cell compartment in PdpnTG mice.

Lymph node cells from two lines of PdpnTG mice and their WT littermates were analyzed by flow cytometry for the frequency and total number of naïve $CD44^{low}CD62L^{hi}$ cells among CD4 T cells (left plots), of $CD44^{hi}CD62L^{low}$ memory T cells (middle plots), and of Foxp3+ Tregs (right plots). Data points represent individual mice. **P<0.05, **P<0.01, ***P<0.001, ****P<0.0001* by unpaired Student's *t*-test.

Figure S7

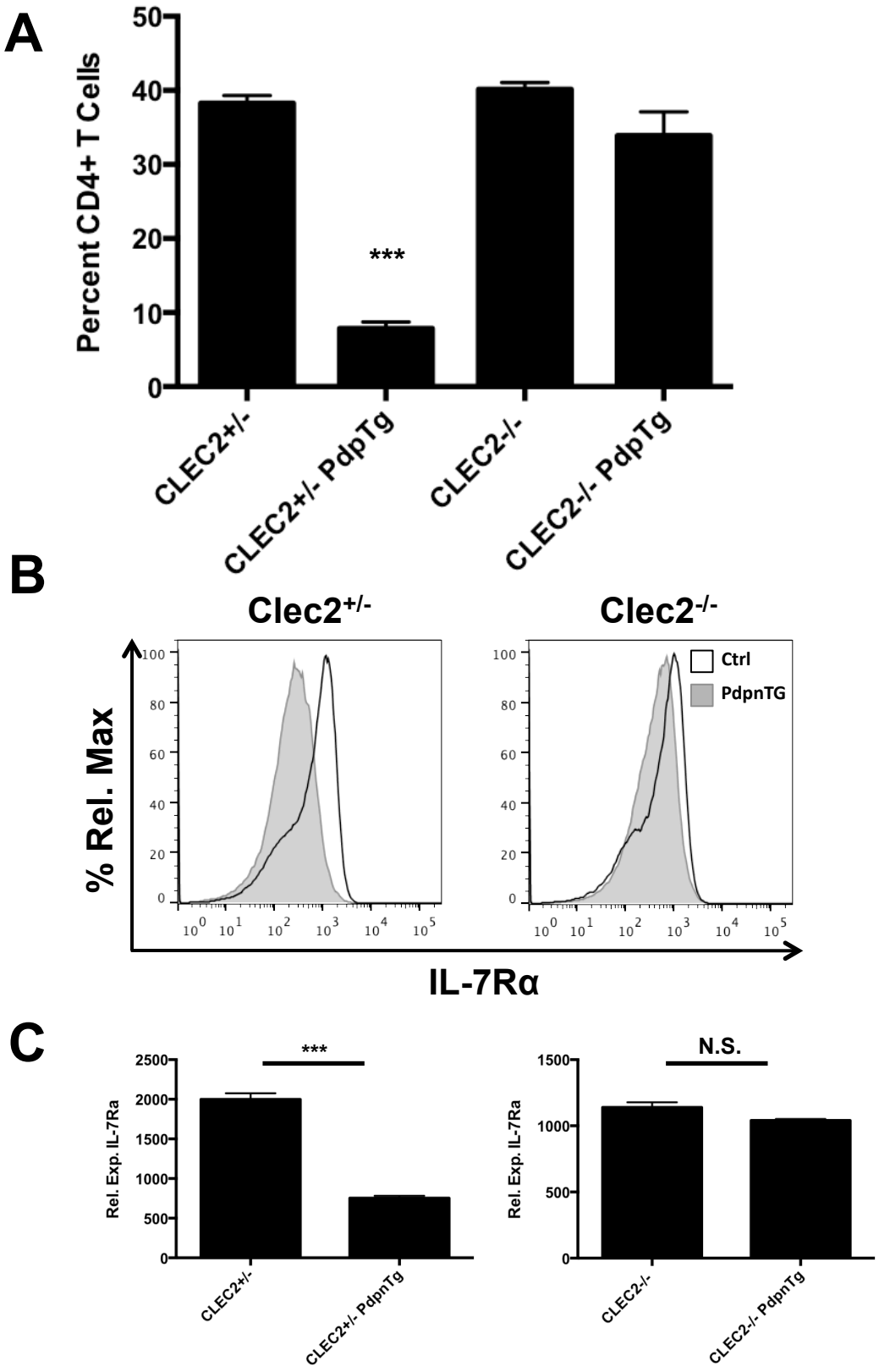
A
Percent CD4+ T Cells
50
40
30
20
10
0
***
CLEC2+/-
CLEC2+/- PdpTg
CLEC2-/-
CLEC2-/- PdpTg
B
Clec2+/-
Clec2-/-
% Rel. Max
100
80
60
40
20
0
Ctrl
PdpnTG
IL-7Rα
C
Rel. Exp. IL-7Ra
2500
2000
1500
1000
500
0
***
CLEC2+/-
CLEC2+/- PdpnTg
1500
1000
500
0
N.S.
CLEC2-/-
CLEC2-/- PdpnTg

Figure S7.Lymphopenia in PdpnTG mice depends on CLEC-2
(A) The frequency of CD4+ T cells from the lymph nodes of $CLEC2^{+/-}$, $CLEC2^{+/-}$ PdpnTg, $CLEC2^{-/-}$, and $CLEC2^{-/-}$ PdpnTg mice was determined by flow cytometry. Data are pooled from two independent experiments with at least three mice per group. **(B)** *IL7Ra* expression on naïve $CD44^{lo}$ CD4 T cells was analyzed by flow cytometry. Data are representative of three mice of each genotype and the two independent experiments. **(C)** *IL7Ra* expression on FACS-sorted $CD44^{lo}$ CD4 T cells was analyzed by qPCR. Data are representative of two independent experiments. ****P<0.001* by unpaired Student's *t*-test.

Table S1: Pdpn-deficient mice develop infiltrates in multiple organs

	Mice with infiltrates in intestine	Mice with infiltrates in lung	Mice with infiltrates in liver	Mice with infiltrates in heart	Mice with infiltrates in CNS
Pdpn-WT	0/4	1/2	0/3	0/3	0/3
Pdpn-KO	4/4	4/4	3/5	0/4	0/4

Table S2: Gene expression analysis in Pdpn+ versus Pdpn- T effectors in the CNS

Gene	Average Fold-difference in Pdpn+ vs. Pdpn- T effectors in the CNS	Gene	Average Fold-difference in Pdpn+ vs. Pdpn- Teffectors in the CNS
p35	-4.84	IL1r1	-1.27
KLF3	-3.88	CXCR6	-1.26
IL-10	-3.45	IL4RA	-1.24
Lef1	-3.34	NFE2L2	-1.23
CREBZF	-3.31	IL2RB	-1.22
Tcf7	-3.18	CTLA4	-1.20
Arg1	-2.91	Sgta	-1.2
SMAD4	-2.85	Pxf/Pex19	-1.19
Adrb2	-2.53	Beta Actin	-1.19

CXCR3	-2.49	STAT4	-1.19
ITGA3	-2.46	CD226	-1.15
tox2	-2.42	Gapdh	-1.14
Il7r	-2.26	TGFB1	-1.08
CCR2	-2.26	STAT5	1.01
IL27R	-2.08	RORc	1.02
Pdcd1l	-2.08	IL-6st	1.04
Zeb1	-2.07	TNFSF9	1.06
SMAD7	-2.01	ID2	1.06
IRF9	-1.98	Il21r	1.08
IL23R	-1.93	Bcl2l1	1.13
GATA3	-1.9	Tubb5	1.16
STAT2	-1.9	Hprt	1.19
DDR1	-1.89	CD39	1.20
MAFF	-1.87	CCL4	1.21
IRF7	-1.83	Il2ra	1.23
Eomes	-1.82	IL1r2	1.23
GABRA1	-1.82	TNFa	1.25
CCR4	-1.81	IL17A	1.26
RUNX2	-1.76	Pdcd1	1.27
Ifnra1	-1.74	lag3	1.28
FOXO1	-1.74	IL6	1.3
L1CAM	-1.74	IL1rn	1.33

SMAD3	-1.73	Rgs16	1.34
NFATc2	-1.71	IRF5	1.39
ICOS	-1.7	IFNg	1.4
TIGIT	-1.69	cbl-b	1.41
Tob	-1.68	pbx3	1.46
KLF7	-1.64	Srxn1	1.48
STAT1	-1.59	TBX21	1.59
RORA	-1.58	CCL5	1.6
CEBPB	-1.57	Serpine2	1.62
Arnt1	-1.57	Il15ra	1.79
Ccnl1	-1.52	SIM1	1.8
CXCR5	-1.52	ChRM1	1.8
Ifnra2	-1.49	Grail	1.8
ETS1	-1.48	CD160	1.8
RUNX1	-1.48	CCR1	1.86
STAT3	-1.47	EBi3	1.87
PLAC8	-1.47	CSF2 (GM-CSF)	1.88
MT2	-1.45	Serpine1	1.9
Bcl2	-1.43	SOCS3	1.93
MAF	-1.43	Gpr56	1.93
NOTCH2	-1.43	CCL20	1.98
LIF	-1.4	SERPINb1b	1.98
NFIL3	-1.38	BATF3	2.11

NFATc1	-1.38	Havcr2	2.13
SGK1	-1.35	IL4	2.17
CMTM6	-1.32	pdpn	2.44
STAT6	-1.31	CXCL3	2.84
IL12RB1	-1.3	CCL12	3.47
IL17F	-1.29	Tmem119	3.69
IL12RB2	-1.29	PROCR	4.92
TGFBR1	-1.28	GZMA	5.81